Inorg. Chem. **2008**, *47*, 10600−10610

Inorganic Chemistry
Article

Self-Assembly of 2D→2D Interpenetrating Coordination Polymers Showing Polyrotaxane- and Polycatenane-like Motifs: Influence of Various Ligands on Topological Structural Diversity

Ya-Qian Lan, Shun-Li Li, Jun-Sheng Qin, Dong-Ying Du, Xin-Long Wang, Zhong-Min Su,* and Qiang Fu*

Institute of Functional Material Chemistry, Key Laboratory of Polyoxometalate Science of Ministry of Education, Faculty of Chemistry, Northeast Normal University, Changchun, 130024, China

Received July 8, 2008

A series of mixed-ligand coordination complexes, namely, $[Cd_2(bimb)_2(L^1)_2]$ (**1**), $[Cd(bpimb)_{0.5}(L^2)(H_2O)]$ (**2**), $[Zn_5(bpib)_2(L^3)_4(OH)_2(H_2O)_2]$ (**3**), $[Zn(bpib)_{0.5}(L^4)]$ (**4**), and $[Cd(bib)(L^4)]$ (**5**), where bimb = 1,4-bis((1*H*-imidazol-1-yl)methyl)benzene, bpimb = 1,4-bis((2-(pyridin-2-yl)-1*H*-imidazol-1-yl)methyl)benzene, bpib = 1,4-bis(2-(pyridin-2-yl)-1*H*-imidazol-1-yl)butane, bib = 1,4-bis(1*H*-imidazol-1-yl)butane, H_2L^1 = 4-((4-(dihydroxymethyl)phenoxy)methyl)benzoic acid, H_2L^2 = 4,4′-methylenebis(oxy)dibenzoic acid, H_2L^3 = 3,3′-methylenebis(oxy)dibenzoic acid, and H_2L^4 = 4,4′-(2,2′-oxybis(ethane-2,1-diyl)bis(oxy))dibenzoic acid, have been synthesized under hydrothermal conditions. Their structures have been determined by single-crystal X-ray diffraction analyses and further characterized by elemental analyses, IR spectra, and thermogravimetric (TG) analyses. In **1**, $(L^1)^{2-}$ anions link the metal−neutral ligand subunits to generate a 2-fold parallel interpenetrating net with the 6^3 topology. In **2**−**4**, neutral ligands connect the various metal−carboxylic ligand subunits to give a 2-fold parallel interpenetrating net with (4,4) topology in **2**, a 2-fold parallel interpenetrating net with (3,6)-connected topology in **3**, and a 3-fold parallel interpenetrating net with (4,4) topology in **4**. Compounds **1**−**4** display both polyrotaxane and polycatenane characters. Compound **5** is a 5-fold parallel interpenetrating net with (4,4) topology. By careful inspection of these structures, we find that different topological structures showing both polyrotaxane and polycatenane characters have been achieved with increase of the carboxylic ligand length. It is believed that various carboxylic ligands and N-donor ligands with different coordination modes and conformations are important for the formation of the different structures. In addition, the luminescent properties of these compounds are discussed.

Introduction

Entangled systems have attracted considerable interest because of their intriguing topological structures and potential applications.[1−4] Among different types of entanglements, interpenetrating networks have been extensively studied.[5] In recent years, the intense interest in coordination polymers has led to more topological types of entanglements being discovered, such as polycatenation, polythreading, and polyknotting, and they are reminiscent of molecular catenanes, rotaxanes, and knots, respectively.[6] According to the research by Ciani and co-workers,[6a] polycatenation differs from interpenetration in that the whole catenated array has a higher dimensionality than that of the component motifs and that each individual motif is catenated only with the surrounding ones and not with all the others. Polythreaded structure is

---

* To whom correspondence should be addressed. E-mail: zmsu@nenu.edu.cn (Z.-M.S), fuq836@nenu.edu.cn (Q.F.). Tel: +86 431 85099108.

(1) (a) *Molecular Catenanes, Rotaxanes and Knots, A Journey Through the World of Molecular Topology*; Sauvage, J. P., Dietrich-Buchecker, C., Eds.; Wiley-VCH: Weinheim, Germany, 1999. (b) Stoddart, J. F. *Acc. Chem. Res.* **2001**, *34*, 410. (c) Kim, K. *Chem. Soc. Rev.* **2002**, *31*, 96. (d) Loeb, S. J. *Chem. Commun.* **2005**, 1511.

(2) (a) Abrahams, B. F.; Batten, S. R.; Grannas, M. J.; Hamit, H.; Hoskins, B. F.; Robson, R. *Angew. Chem., Int. Ed.* **1999**, *38*, 1475. (b) Biradha, K.; Fujita, M. *Chem. Commun.* **2002**, 1866. (c) Li, Y. H.; Su, C. Y.; Goforth, A. M.; Shimizu, K. D.; Gray, K. D.; Smith, M. D.; zur Loye, H. C. *Chem. Commun.* **2003**, 1630. (d) Tong, M. L.; Chen, X. M.; Batten, S. R. *J. Am. Chem. Soc.* **2003**, *125*, 16170. (e) Moulton, B.; Abourahma, H.; Bradner, M. W.; Lu, J.; McManus, G. J.; Zaworotko, M. J. *Chem. Commun.* **2003**, 1342.

(3) (a) Long, D. L.; Hill, R. J.; Blake, A. J.; Champness, N. R.; Hubberstey, P.; Wilson, C.; Schröder, M. *Chem.*−*Eur. J.* **2005**, *11*, 1384. (b) He, J.; Yin, Y. G.; Wu, T.; Li, D.; Huang, X. C. *Chem. Commun.* **2006**, 2845. (c) Cheng, A. L.; Liu, N.; Yue, Y. F.; Jiang, Y. W.; Gao, E. Q.; Yan, C. H.; He, M. Y. *Chem. Commun.* **2007**, 407.

10.1021/ic801275w CCC: $40.75

characterized by the presence of closed loops, as well as of elements that can thread through the loops, and can be considered as extended periodic analogues of molecular rotaxanes and pseudorotaxanes, depending on the "ideal" possibility of being extricated. To date, although some polycatenated or polythreaded coordination polymers have been reported,[7,8] the topological frameworks containing two kinds of entangled motifs in one compound are still quite rare. Only a few fascinating structures showing both polyrotaxane and polycatenane characters have been observed.[9] However, there is an unfavorable lack of detailed investigation on different topological structures in above-mentioned nets, such as other topological nets and various interpenetrating ones.

As shown above, it is a great challenge not only to synthesize entangled frameworks having both polyrotaxane and polycatenane characters but also to achieve different topological structures in the aforementioned system. To achieve this aim, we have designed and synthesized a series of flexible N-donor ligands (1,4-bis((1*H*-imidazol-1-yl)methyl)benzene (bimb), 1,4-bis((2-(pyridin-2-yl)-1*H*-imidazol-1-yl)methyl)benzene (bpimb), 1,4-bis(2-(pyridin-2-yl)-1*H*-imidazol-1-yl)butane (bpib), and 1,4-bis(1*H*-imidazol-1-yl)butane (bib)) and multicarboxylic bridging ligands (4-((4-(dihydroxymethyl)phenoxy)methyl)benzoic acid (H_2L^1), 4,4′-methylenebis(oxy)dibenzoic acid (H_2L^2), 3,3′-methylenebis(oxy)dibenzoic acid (H_2L^3), and 4,4′-(2,2′-oxybis(ethane-2,1-diyl)bis(oxy))dibenzoic acid (H_2L^4)) based on the following considerations: (i) The use of conformationally nonrigid ligands can favor the formation of interesting motifs with peculiar features like new topologies and entanglements (including polycatenanes and polyrotaxanes).[6a,10] (ii) The carboxylic bridging ligands contain the flexible -CH_2- or -O-CH_2- spacer. Therefore, the two phenyl rings can freely twist around the -CH_2- group or -O-CH_2- to meet the requirements of the coordination geometries of metal atoms in the assembly process. Conformational changes of flexible ligands can more easily give unusual entanglements involving a molecular unit with loops and insertion of a linear rod through those loops. (iii) From H_2L^1 to H_2L^2 to H_2L^3 to H_2L^4 (Chart 1), the different lengths of carboxylic bridging ligands maybe benefit the formation of different topological structures. Because an accurate prediction of the final structure is impossible, the exploration of the influencing factors for the ultimate structures is not trivial. In this paper, we have tried different synthetic conditions and performed many experiments. Fortunately, compounds $[Cd_2(bimb)_2(L^1)_2]$ (**1**), $[Cd(bpimb)_{0.5}(L^2)(H_2O)]$ (**2**), $[Zn_5(bpib)_2(L^3)_4(OH)_2(H_2O)_2]$ (**3**), $[Zn(bpib)_{0.5}(L^4)]$ (**4**), and $[Cd(bib)(L^4)]$ (**5**) have been successfully isolated by hydrothermal methods. In addition, the infrared spectra, thermogravimetric analyses, and luminescent properties of these compounds have been investigated in detail.

Chart 1. The Carboxylate Ligands and Neutral Ligands in **1**−**5**

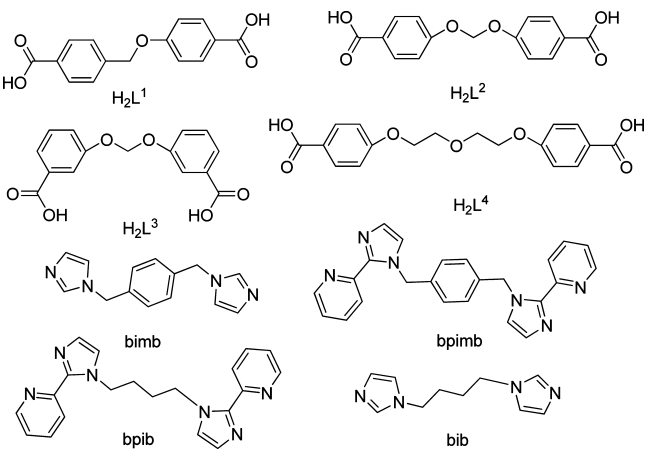

Experimental Section

General Procedures. Chemicals were purchased from commercial sources and used without further purification. Ligands bimb, bpimb, bpib, and bib were prepared according to literature procedures.[11]

Synthesis of H_2L^1. A mixture of ethyl 4-hydroxybenzoate (8.30 g, 50 mmol) and NaOH (2.00 g, 50 mmol) in DMSO (20 mL) was stirred at 5 °C for 2 h, then 4-(chloromethyl)benzonitrile (7.55 g, 50 mmol) was added. The mixture was cooled to room temperature

---

(4) (a) Miller, J. S. *Adv. Mater.* **2001**, *13*, 525. (b) Janiak, C. *Dalton Trans.* **2003**, 2781. (c) Eddaoudi, M.; Kim, J.; Rosi, N.; Vodak, D.; Wachter, J.; O'Keeffe, M.; Yaghi, O. M. *Science* **2002**, *295*, 469. (d) Kesanli, B.; Cui, Y.; Smith, M. R.; Bittner, E. W.; Bockrath, B. C.; Lin, W. *Angew. Chem., Int. Ed.* **2005**, *44*, 72. (e) Sun, D. F.; Ma, S. Q.; Ke, Y. X.; Collins, D. J.; Zhou, H. C. *J. Am. Chem. Soc.* **2006**, *128*, 3896. (f) Chen, B. L.; Ma, S. Q.; Zapata, F.; Fronczek, F. R.; Lobkovsky, E. B.; Zhou, H. C. *Inorg. Chem.* **2007**, *46*, 1233. (g) Zhang, J. P.; Horike, S.; Kitagawa, S. *Angew. Chem., Int. Ed.* **2007**, *46*, 889. (h) Maji, T.; Matsuda, R.; Kitagawa, S. *Nat. Mater.* **2007**, *6*, 142.

(5) (a) Batten, S. R.; Robson, R. *Angew. Chem., Int. Ed.* **1998**, *37*, 1460. (b) Batten, S. R. *CrystEngComm* **2001**, *3*, 67.

(6) (a) Carlucci, L.; Ciani, G.; Proserpio, D. M. *Coord. Chem. Rev.* **2003**, *246*, 247. (b) Carlucci, L.; Ciani, G.; Proserpio, D. M. *CrystEngComm* **2003**, *5*, 269. (c) Wang, X. L.; Qin, C.; Wang, E. B.; Li, Y. G.; Su, Z. M.; Xu, L.; Carlucci, L. *Angew. Chem., Int. Ed.* **2005**, *44*, 5824.

(7) (a) Carlucci, L.; Ciani, G.; Moret, M.; Proserpio, D. M.; Rizzato, S. *Angew. Chem., Int. Ed.* **2000**, *39*, 1506. (b) Li, B. L.; Peng, Y. F.; Li, B. Z.; Zhang, Y. *Chem. Commun.* **2005**, 2333. (c) Carlucci, L.; Ciani, G.; Maggini, M.; Proserpio, D. M. *Cryst. Growth Des.* **2008**, *8*, 162. (d) Vishweshwar, P.; Beauchamp, D. A.; Zaworotko, M. J. *Cryst. Growth Des.* **2006**, *6*, 2429. (e) Carlucci, L.; Ciani, G.; Proserpio, D. M. *Chem. Commun.* **2004**, 380. (f) Lu, J. Y.; Babb, A. M. *Chem. Commun.* **2001**, 821. (g) Jiang, Y. C.; Lai, Y. C.; Wang, S. L.; Lii, K. H. *Inorg. Chem.* **2001**, *40*, 5320. (h) Shin, D. M.; Lee, I. S.; Chung, Y. K.; Lah, M. S. *Chem. Commun.* **2003**, 1036. (i) Shin, D. M.; Lee, I. S.; Cho, D.; Chung, Y. K. *Inorg. Chem.* **2003**, *42*, 7722. (j) Carlucci, L.; Ciani, G.; Proserpio, D. M.; Spadacini, L. *CrystEngComm* **2004**, *6*, 96. (k) Zhu, H.-F.; Fan, J.; Okamura, T.-a.; Sun, W.-Y.; Ueyama, N. *Cryst. Growth Des.* **2005**, *5*, 289. (l) Sagué, J. L.; Fromm, K. M. *Cryst. Growth Des.* **2006**, *6*, 1566. (m) Hoskins, B. F.; Robson, R.; Slizys, D. A. *J. Am. Chem. Soc.* **1997**, *119*, 2952. (n) Carlucci, L.; Ciani, G.; Proserpio, D. M. *Cryst. Growth Des.* **2005**, *5*, 37.

(8) (a) Carlucci, L.; Ciani, G.; Proserpio, D. M. *Chem. Commun.* **1999**, 449. (b) Du, M.; Jiang, X.-J.; Zhao, X.-J. *Chem. Commun.* **2005**, 5521. (c) Qin, C.; Wang, X. L.; Carlucci, L.; Tong, M. L.; Wang, E. B.; Hu, C. W.; Xu, L. *Chem. Commun.* **2004**, 1876. (d) Wang, X. L.; Qin, C.; Wang, E. B.; Xu, L. *Cryst. Growth Des.* **2006**, *6*, 2061. (e) Du, M.; Jiang, X. J.; Zhao, X. J. *Inorg. Chem.* **2007**, *46*, 3984. (f) Lan, Y. Q.; Li, S. L.; Wang, X. L.; Su, Z. M.; Shao, K. Z.; Wang, E. B. *Chem. Commun.* **2007**, 4863. (g) Lan, Y. Q.; Li, S. L.; Wang, X. L.; Shao, K. Z.; Su, Z. M.; Wang, E. B. *Inorg. Chem.* **2008**, *47*, 529.

(9) (a) Goodgame, D. M. L.; Menzer, S.; Smith, A. M.; Williams, D. J. *Angew. Chem., Int. Ed. Engl.* **1995**, *34*, 574. (b) Hoskins, B. F.; Robson, R.; Slizys, D. A. *Angew. Chem., Int. Ed. Engl.* **1997**, *36*, 2336. (c) Yang, J.; Ma, J.-F.; Batten, S. R.; Su, Z.-M. *Chem. Commun.* **2008**, 2233. (d) Luo, F.; Yang, Y.-T.; Che, Y.-X.; Zheng, J.-M. *CrystEngComm* **2008**, 981. (e) Wang, G.-H.; Li, Z.-G.; Jia, H.-Q.; Hu, N.-H.; Xu, J.-W. *Cryst. Growth Des.* **2008**, *8*, 1932. (f) Qin, C.; Wang, X.-L.; Wang, E.-B.; Su, Z.-M. *Inorg. Chem.* **2008**, *47*, 5555.

after stirring at 50 °C for 24 h and then poured into 200 mL of water. A yellow solid of ethyl 4-(4-cyanobenzyloxy)benzoate formed immediately, which was isolated by filtration in 94% yield after drying in air.

A mixture of ethyl 4-(4-cyanobenzyloxy)benzoate (14.07 g, 50 mmol) and KOH (11.20 g, 200 mmol) in H_2O (200 mL) was stirred at 100 °C for 15 h, and was cooled to room temperature. Then the mixture was adjusted to pH $\approx$ 5 with HCl (1.0 mol$\cdot$L^{-1}), and a white solid of H_2L^1 formed immediately, which was isolated by filtration in 60% yield after drying in air. IR (cm^{-1}): 3743 (w), 3442 (w), 2985 (w), 2546 (w), 2362 (m), 1681 (s), 1606 (s), 1577 (m), 1514 (m), 1425 (s), 1385 (s), 1292 (s), 1252 (s), 1172 (s), 1047 (m), 949 (w), 854 (w), 765 (m).

Syntheses of H_2L^2, H_2L^3, and H_2L^4. A mixture of ethyl 4-hydroxybenzoate (8.30 g, 50 mmol) and NaOH (2.00 g, 50 mmol) in DMSO (20 mL) was stirred at 5 °C for 2 h, and then dichloromethane (2.12 g, 25 mmol) was added. The mixture was stirred at 5 °C for 48 h and then poured into 200 mL of water. A white solid of diethyl 4,4′-methylenebis(oxy)dibenzoate formed immediately, which was isolated by filtration in 91% yield after drying in air.

A mixture of diethyl 4,4′-methylenebis(oxy)dibenzoate (17.20 g, 50 mmol) and KOH (11.20 g, 200 mmol) in H_2O (200 mL) was stirred at 100 °C for 8 h and was cooled to room temperature. Then the mixture was adjusted to pH $\approx$ 5 with HCl (1.0 mol$\cdot$L^{-1}), and a white solid of H_2L^2 formed immediately, which was isolated by filtration in 75% yield after drying in air. IR (cm^{-1}): 3897 (w), 3743 (m), 2982 (w), 1716 (s), 1645 (m), 1608 (s), 1539 (m), 1510 (s), 1462 (m), 1369 (m), 1314 (s), 1275 (s), 1218 (s), 1168 (s), 1105 (m), 1025 (s), 849 (w), 767 (m).

H_2L^3 was prepared in the same way as H_2L^2 by using the corresponding ethyl 3-hydroxybenzoate instead of ethyl 4-hydroxybenzoate. IR (cm^{-1}): 3887 (w), 3740 (m), 2985 (w), 1726 (s), 1645 (m), 1608 (s), 1549 (m), 1512 (s), 1462 (m), 1318(s), 1274 (s), 1218 (s), 1172 (s), 1105 (m), 1035 (s), 849 (w), 767 (m).

H_2L^4 was prepared in the same way as H_2L^2 by using the corresponding bis(2-chloroethyl)ether instead of dichloromethane. IR (cm^{-1}): 3827 (m), 3745 (m), 2985 (w), 1715 (s), 1683 (s), 1606 (s), 1577 (m), 1508 (s), 1457 (m), 1366 (m), 1278 (s), 1171 (m), 1106 (s), 1052 (m), 957 (w), 851 (w), 768 (w).

Synthesis of $[Cd_2(bimb)_2(L^1)_2]$ (1). A mixture of bimb (0.24 g, 1.00 mmol), H_2L^1 (0.27 g, 1.0 mmol), $Cd(OAc)_2\cdot 2H_2O$ (0.27 g, 1.00 mmol), NaOH (0.08 g, 2.00 mmol), and H_2O (10 mL) was stirred for 1 h and then sealed in a 25 mL Teflon-lined stainless steel container. The container was heated to 150 °C and held at that temperature for 72 h, then cooled to 100 °C at a rate of 10 °C$\cdot$h^{-1}, held for 8 h, and further cooled to 30 °C at a rate of 5 °C$\cdot$h^{-1}. Colorless crystals of **1** were collected in 72.7% yield based on $Cd(OAc)_2\cdot 2H_2O$. Anal. Calcd for $C_{58}H_{48}Cd_2N_8O_{10}$ (1241.84): C, 56.09; H, 3.90; N, 9.02. Found: C, 56.87; H, 3.86; N, 8.99%. IR (cm^{-1}): 3861 (s), 3741 (s), 3120 (m), 2882 (s), 2817 (s), 1836 (w), 1751 (w), 1707 (w), 1516 (m), 1395 (m), 1223 (w), 1142 (w), 1000 (m), 849 (w), 774 (w), 673 (m).

Synthesis of $[Cd(bpimb)_{0.5}(L^2)(H_2O)]$ (2). A mixture of bpimb (0.39 g, 1.00 mmol), H_2L^2 (0.29 g, 1.0 mmol), $Cd(OAc)_2\cdot 2H_2O$ (0.27 g, 1.00 mmol), NaOH (0.08 g, 2.00 mmol), and H_2O (10 mL) was stirred for 1 h and then sealed in a 25 mL Teflon-lined stainless steel container. The container was heated to 150 °C and held at that temperature for 72 h, then cooled to 100 °C at a rate of 10 °C$\cdot$h^{-1}, held for 8 h, and further cooled to 30 °C at a rate of 5 °C$\cdot$h^{-1}. Colorless crystals of **2** were collected in 69.7% yield based on $Cd(OAc)_2\cdot 2H_2O$. Anal. Calcd for $C_{27}H_{22}CdN_3O_7$ (612.88): C, 52.91; H, 3.62; N, 6.86. Found: C, 52.85; H, 3.55; N, 6.93%. IR (cm^{-1}): 3731 (s), 3121 (s), 2883 (w), 1836 (w), 1798 (w), 1751 (w), 1707 (w), 1645 (w), 1596 (m), 1477 (s), 1423 (s), 1394 (s), 1298 (s), 1205 (m), 1153 (m), 1096 (m), 999 (m), 942 (w), 853 (w), 782 (m).

Synthesis of $[Zn_5(bpib)_2(L^3)_4(OH)_2(H_2O)_2]$ (3). A mixture of bpib (0.34 g, 1.00 mmol), H_2L^3 (0.29 g, 1.00 mmol), $Zn(OAc)_2\cdot 2H_2O$ (0.22 g, 1.00 mmol), NaOH (0.08 g, 2.00 mmol), and H_2O (10 mL) was stirred for 1 h and then sealed in a 25 mL Teflon-lined stainless steel container. The container was heated to 150 °C and held at that temperature for 72 h, then cooled to 100 °C at a rate of 10 °C$\cdot$h^{-1}, held for 8 h, and further cooled to 30 °C at a rate of 5 °C$\cdot$h^{-1}. Colorless crystals of **3** were collected in 64.5% yield based on $Zn(OAc)_2\cdot 2H_2O$. Anal. Calcd for $C_{100}H_{86}N_{12}O_{28}Zn_5$ (2230.66): C, 53.84; H, 3.89; N, 7.53. Found: C, 53.79; H, 3.78; N, 7.46%. IR (cm^{-1}): 3731 (w), 3671 (w), 3116 (m), 2875 (m), 2788 (m), 1609 (m), 1568 (s), 1478 (s), 1445 (s), 1386 (s), 1282 (m), 1209 (s), 1167 (w), 1090 (w), 1017 (s), 896 (w), 770 (s), 674 (m).

Synthesis of $[Zn(bpib)_{0.5}(L^4)]$ (4). A mixture of bpib (0.34 g, 1.00 mmol), H_2L^4 (0.35 g, 1.00 mmol), $Zn(OAc)_2\cdot 2H_2O$ (0.22 g, 1.00 mmol), NaOH (0.08 g, 2.00 mmol), and H_2O (10 mL) was stirred for 1 h and then sealed in a 25 mL Teflon-lined stainless steel container. The container was heated to 150 °C and held at that temperature for 72 h, then cooled to 100 °C at a rate of 10 °C$\cdot$h^{-1}, held for 8 h, and further cooled to 30 °C at a rate of 5 °C$\cdot$h^{-1}. Colorless crystals of **4** were collected in 77.6% yield based on $Zn(OAc)_2\cdot 2H_2O$. Anal. Calcd for $C_{28}H_{26}N_3O_7Zn$ (581.89): C, 57.79; H, 4.50; N, 7.22. Found: C, 57.83; H, 4.37; N, 7.39%. IR (cm^{-1}): 3732 (w), 3120 (m), 2940 (m), 2882 (m), 2828 (m), 1634 (s), 1601 (s), 1500 (s), 1411 (s), 1347 (s), 1252 (s), 1168 (m), 1130 (s), 1054 (s), 948 (m), 922 (m), 854 (w), 784 (m), 742 (w), 657 (w).

Synthesis of $[Cd(bib)(L^4)]$ (5). A mixture of bib (0.19 g, 1.00 mmol), H_2L^4 (0.35 g, 1.00 mmol), $Cd(OAc)_2\cdot 2H_2O$ (0.27 g, 1.00 mmol), NaOH (0.08 g, 2.00 mmol), and H_2O (10 mL) was stirred for 1 h and then sealed in a 25 mL Teflon-lined stainless steel container. The container was heated to 150 °C and held at that temperature for 72 h, then cooled to 100 °C at a rate of 10 °C$\cdot$h^{-1}, held for 8 h, and further cooled to 30 °C at a rate of 5 °C$\cdot$h^{-1}. Colorless crystals of **5** were collected in 78.4% yield based on $Cd(OAc)_2\cdot 2H_2O$. Anal. Calcd for $C_{28}H_{30}CdN_4O_7$ (646.96): C, 51.98; H, 4.67; N, 8.66. Found: C, 52.02; H, 4.79; N, 8.74.% IR (cm^{-1}): 3742 (s), 3104 (s), 2872 (w), 1706 (w), 1596 (s), 1515 (s), 1453 (m), 1393 (s), 1298 (w), 1239 (m), 1162 (w), 1107 (w), 937 (m), 852 (m), 777 (m), 692 (m).

Physical Measurements. The C, H, and N elemental analysis was conducted on a Perkin-Elmer 240C elemental analyzer. The FT-IR spectra were recorded from KBr pellets in the range of 4000−400 cm^{-1} on a Mattson Alpha-Centauri spectrometer. TGA was performed on a Perkin-Elmer TG-7 analyzer heated from room temperature to 700 °C under nitrogen. The solid-state emission/excitation spectra were recorded on a Varian Cary Eclipse spectrometer at room temperature.

---

(10) (a) Carlucci, L.; Ciani, G.; Proserpio, D. M. *Networks, Topologies, and Entanglements in Making Crystals by Design - Methods, Techniques and Applications*; Braga, D., Grepioni, F., Eds.; Wiley-VCH: Weinheim, Germany, 2007; Chapter 1.3. (b) Carlucci, L.; Ciani, G.; Maggini, S.; Proserpio, D. M. *CrystEngComm* **2008**, 1191.

(11) (a) Li, S.-L.; Lan, Y.-Q.; Ma, J.-F.; Yang, J.; Wei, G.-H.; Zhang, L.-P.; Su, Z.-M. *Cryst. Growth Des.* **2008**, *8*, 675. (b) Reeder, K. A.; Dose, E. V.; Wilson, L. J. *Inorg. Chem.* **1978**, *17*, 1071. (c) Chiswell, B.; Lions, F.; Morris, B. S. *Inorg. Chem.* **1964**, *3*, 110. (d) Lan, Y.-Q.; Fu, Y.-M.; Shao, K.-Z.; Su, Z.-M. *Acta Crystallogr.* **2006**, *E62*, 2586. (e) Li, S.-L.; Lan, Y.-Q.; Ma, J.-F.; Fu, Y.-M.; Yang, J.; Ping, G.-J.; Liu, J.; Su, Z.-M. *Cryst. Growth Des.* **2008**, *8*, 1610.

Table 1. Crystal Data and Structure Refinements for Compounds **1**−**5**

	1	**2**	**3**	**4**	**5**
formula	$C_{58}H_{48}Cd_2N_8O_{10}$	$C_{27}H_{22}CdN_3O_7$	$C_{100}H_{86}N_{12}O_{28}Zn_5$	$C_{28}H_{26}N_3O_7Zn$	$C_{28}H_{30}CdN_4O_7$
fw	1241.84	612.88	2230.66	581.89	646.96
crystal system	triclinic	triclinic	triclinic	triclinic	monoclinic
space group	$P\bar{1}$	$P\bar{1}$	$P\bar{1}$	$P\bar{1}$	$P2_1/n$
a (Å)	9.7860(6)	10.3930(5)	11.5890(4)	8.2200(3)	7.1680(3)
b (Å)	14.7460(9)	11.0290(5)	11.7730(4)	12.4460(5)	24.8870(6)
c (Å)	19.8720(12)	12.0990(5)	19.6900(7)	13.5470(5)	15.4390(7)
α (deg)	100.7460(10)	110.6250(10)	94.4840(10)	98.6910(6)	90
β (deg)	97.9240(10)	105.6710(10)	105.2900(10)	98.8260(10)	91.0140(10)
γ (deg)	100.6960(10)	93.4570(10)	114.1670(10)	109.2600(10)	90
V (Å^3)	2723.8(3)	1230.97(10)	2310.75(14)	1262.29(8)	2753.73(18)
Z	2	2	1	2	4
D_{calcd} [g cm^{-3}]	1.514	1.654	1.603	1.531	1.561
F(000)	1256	618	1144	602	1320
reflns collected /unique	13923/9522	7599/5501	14529/10619	7818/5660	16942/6614
R(int)	0.0194	0.0115	0.0233	0.0091	0.0253
GOF on F^2	1.042	1.034	1.031	1.051	1.035
$R_1{}^a$ [$I > 2\sigma(I)$]	0.0458	0.0358	0.0500	0.0271	0.0390
$wR_2{}^b$	0.0976	0.0950	0.1212	0.0687	0.0878
largest residuals [e Å^{-3}]	0.744/−0.480	0.910/−0.994	1.440/−0.559	0.341/−0.312	0.904/−0.468

[a] $R_1 = \sum||F_o| - |F_c||/\sum|F_o|$. [b] $wR_2 = |\sum w(|F_o|^2 - |F_c|^2)|/\sum|w(F_o{}^2)^2|^{1/2}$.

X-ray Crystallography. Single-crystal X-ray diffraction data for compounds **1**−**5** were recorded on a Bruker Apex CCD diffractometer with graphite-monochromated Mo Kα radiation ($\lambda = 0.71073$ Å) at 293 K. Absorption corrections were applied using the multiscan technique. All the structures were solved by direct methods using SHELXS-97[12] and refined by full-matrix least-squares techniques using the SHELXL-97 program[13] within WINGX.[14] Non-hydrogen atoms were refined with anisotropic temperature parameters. The hydrogen atoms of the organic ligands were refined on idealized positions. H atoms of water molecules were located from different Fourier maps. The detailed crystallographic data and structure refinement parameters for **1**−**5** are summarized in Table 1.

Results

Structural Description of 1. As shown in Figure 1a, the structure of **1** contains two kinds of unique Cd^{II} atoms, two kinds of unique $(L^1)^{2-}$ anions, and two kinds of unique bimb ligands. The Cd1 cation shows an octahedral coordination geometry $\{CdN_2O_4\}$, which is completed by four carboxylate oxygen atoms from two $(L^1)^{2-}$ anions, and two nitrogen atoms from two bimb ligands. The Cd2 cation is five-coordinated by three carboxylate oxygen atoms from two $(L^1)^{2-}$ anions, and two nitrogen atoms from two bimb ligands, showing a trigonal bipyramidal geometry $\{CdN_2O_3\}$. The Cd^{II}−O and Cd^{II}−N distances are quite similar to normal Cd^{II}−O and Cd^{II}−N distances (Table S1, Supporting Information).[15] A pair of bimb ligands in the bis-monodentate bridge adjacent Cd^{II} atoms to give a 26-membered ring [Cd(bimb)$_2$Cd] with the dimensions 9.265 Å × 11.708 Å (Figure S1a, Supporting Information), which is further linked by $(L^1)^{2-}$ ligands in the monobidentate and bis-bidentate modes with T conformations (considering the relative orientations T = trans, G = gauche) to give a 2D undulated layer (Figure 1b), showing a rectangular window with the dimensions 17.460 Å × 28.589 Å. So six Cd^{II} ions are linked by four bimb and four $(L^1)^{2-}$ ligands to form a large rectangular 86-membered ring [Cd$_6$(bimb)$_2$(L^1)$_4$] with the distances for each edge and diagonal of 17.460, 28.589, 29.199, and 37.307 Å, respectively (Figure S1b, Supporting Information). If each [Cd(bimb)$_2$Cd] 26-membered ring is considered as a 3-connected node, the structure of **1** exhibits a 6^3 topology (Figure 1c).

In order to minimize the big void cavities and stabilize the framework, the potential voids formed by a single 2D network show incorporation of another identical network, thus giving a 2-fold parallel interpenetrating network (Figure 1d and Figure S1c, Supporting Information). To further study the structure, each [Cd(bimb)$_2$Cd] 26-membered loop of each layer is threaded by the rod of one $(L^1)^{2-}$ ligand from the other layer, and vice versa. In addition, the polyrotaxane nature of this net is evident in the presence of catenated rings by the [Cd(bimb)$_2$Cd] 26-membered ring and the [Cd$_6$(bimb)$_2$(L^1)$_4$] 86-membered ring from adjacent layers, which makes the nontrivial topology of the entanglement (Figure 1e,f). So the structure of **1** shows both polyrotaxane and polycatenane characteristics.

Structural Description of 2. When H_2L^1 is replaced with longer H_2L^2 and bimb is replaced with bpimb, a similar parallel interpenetrating 2D structure, **2**, has been obtained. The structure of **2** contains one kind of Cd^{II} atom, one kind of bpimb ligand, and one kind of $(L^2)^{2-}$ anion. Cd1 is coordinated by three carboxylate oxygen atoms from different $(L^2)^{2-}$ anions, two nitrogen atoms from one bpimb ligand, and one coordinating water molecule, showing an octahedral geometry $\{CdN_2O_4\}$ (Figure 2a). Different from **1**, $(L^2)^{2-}$

---

(12) Sheldrick, G. M. *SHELXS-97, Programs for X-ray Crystal Structure Solution*; University of Göttingen: Göttingen, Germany, 1997.

(13) Sheldrick, G. M. *SHELXL-97, Programs for X-ray Crystal Structure Refinement*; University of Göttingen: Göttingen, Germany, 1997.

(14) Farrugia, L. J. *WINGX, A Windows Program for Crystal Structure Analysis*; University of Glasgow: Glasgow, UK, 1988.

(15) (a) Dai, J.-C.; Wu, X.-T.; Fu, Z.-Y.; Cui, C.-P.; Hu, S.-M.; Du, W.-X.; Wu, L.-M.; Zhang, H.-H.; Sun, R.-Q. *Inorg. Chem.* **2002**, *41*, 1391. (b) Wang, R.; Hong, M.; Luo, J.; Cao, R.; Weng, J. *Chem. Commun.* **2003**, 1018. (c) Luan, X.-J.; Cai, X.-H.; Wang, Y.-Y.; Li, D.-S.; Wang, C.-J.; Liu, P.; Hu, H.-M.; Shi, Q.-Z.; Peng, S.-M. *Chem.—Eur. J.* **2006**, *12*, 6281. (d) Paz, F. A. A.; Klinowski, J. *Inorg. Chem.* **2004**, *43*, 3948. (e) Zou, R.-Q.; Bu, X.-H.; Zhang, R.-H. *Inorg. Chem.* **2004**, *43*, 5382. (f) Suresh, E.; Boopalan, K.; Jasra, R. V.; Bhadbhade, M. M. *Inorg. Chem.* **2001**, *40*, 4078.

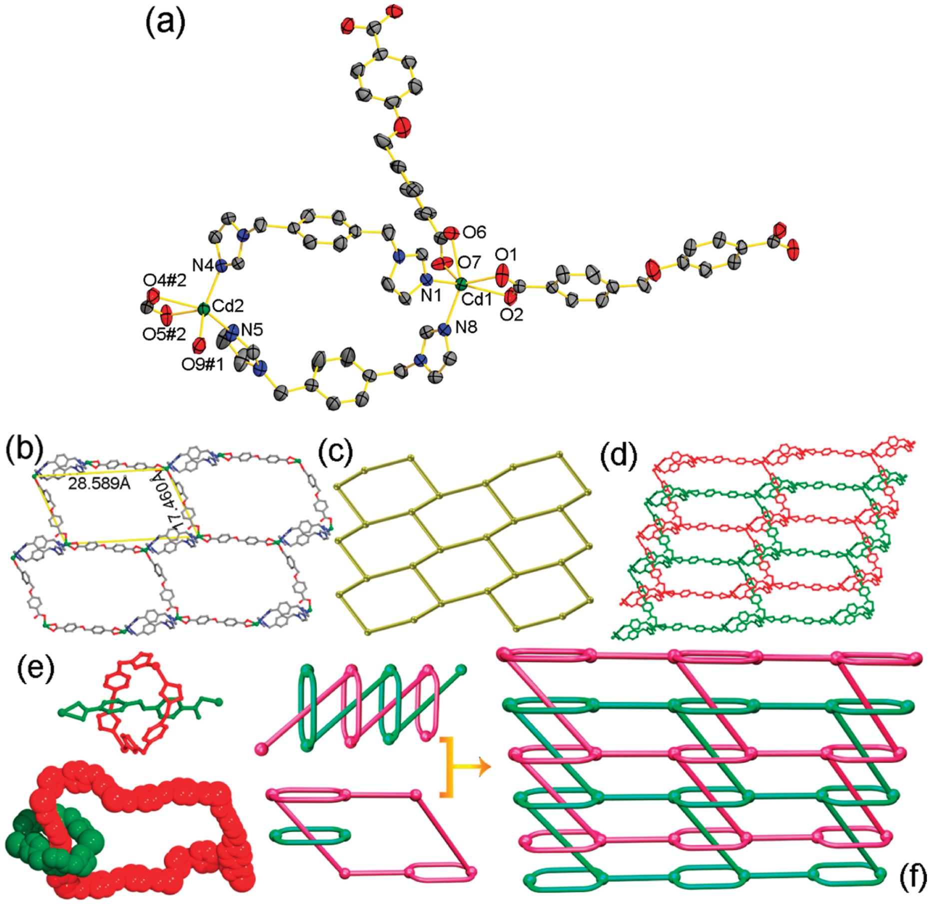

Figure 1. (a) Coordination environment of Cd^{II} atoms in **1** with the ellipsoids drawn at the 30% probability level; hydrogen atoms were omitted for clarity; (b) ball-and-stick representation of the sheet-like structure of compound **1**; (c) schematic view of the 6^3 topology of **1**; (d) ball-and-stick representation of interlocked nets; (e) the polyrotaxane and polycatenane motifs in **1**; (f) schematic description of the interpenetrating nets of **1**.

anions connect Cd^{II} ions with the mono-and-bis(mono)-dentate coordination mode in the GG conformation to generate a double chain, in which there exists a rectangular 32-membered ring $[Cd(L^2)_2Cd]$ (Figure S2a) with distances for each edge and diagonal of 9.206, 9.425, 12.348, and 13.953 Å, respectively. The adjacent double chains are pillared by bpimb ligands with bis-bidentate coordination mode to form an undulated sheet (Figure 2b), showing a rectangular window with the dimensions 14.691 Å × 15.604 Å. Within the layer, there is a large 86-membered ring $[Cd_4(bpimb)_2(L^2)_2]$ with corresponding distances of 12.414, 14.691, 17.417, and 20.893 Å (Figure S2b, Supporting Information). From the topological view, if each $[Cd(L^2)_2Cd]$ ring is considered as a 4-connected node, the structure of **2** exhibits a (4,4) topology (Figure 2c).

Similar to compound **1**, two identical layers penetrate each other in parallel interpenetrating modes to give a 2-fold parallel interpenetrating network (Figure 2d and Figure S2c, Supporting Information), which shows both polyrotaxane and polycatenane character. Each bpimb as a rod threads the $[Cd(L^2)_2Cd]$ loop from the adjacent layers and two kinds of loops of the $[Cd(L^2)_2Cd]$ ring and the $[Cd_4(bpimb)_2(L^2)_2]$ ring from adjacent sheets catenate each other (Figure 2e,f).

Compounds **1** and **2** are 2-fold parallel interpenetrating networks and exhibit both polyrotaxane and polycatenane character. Comparison of two structures shows that the distinction between them is the different compositions for the smaller loops, such as $[Cd(bimb)_2Cd]$ in **1** and $[Cd(L^2)_2Cd]$ in **2**, which are connected to form final structures with various topologies. In the literature, such nets with 6^3 and (4,4) topologies containing both polyrotaxane and polycatenane character are quite rare.[9a−e]

Structural Description of 3. When H_2L^3 with different angular character replaced H_2L^2 and the flexible bpib ligand is selected instead of bpimb, a particularly fascinating 2D 2-fold structure of **3** has been obtained. There are three kinds of unique Zn^{II} atoms, two kinds of unique $(L^3)^{2-}$ anions, and one kind of bpib ligand (Figure 3a). The Zn1 cation shows a trigonal bipyramidal geometry $\{ZnN_2O_3\}$, which is surrounded by two carboxylate oxygen atoms from two $(L^3)^{2-}$ anions, one $(OH)^-$ group, and two nitrogen atoms from one bpib ligand. The Zn2 cation is five-coordinated by two carboxylate oxygen atoms from different $(L^3)^{2-}$ anions, two nitrogen atoms from the bpib ligand, and one water molecule, showing a trigonal bipyramidal geometry $\{ZnN_2O_3\}$. Zn3 exhibits an octahedral coordination geometry with four carboxylate atoms from different $(L^3)^{2-}$ anions and two $(OH)^-$ groups. The $Zn^{II}-O$ and $Zn^{II}-N$ distances are quite similar to normal $Zn^{II}-O$ and $Zn^{II}-N$ distances.[16] Two types of $(L^3)^{2-}$ anions with mono-and-bis(mono)-dentate coordination modes in the GG conformations connect Zn^{II} ions to give a double chain. Within this chain, two adjacent Zn1 atoms and one Zn3 atom are bridged by four carboxylate groups and two $(OH)^-$ groups to give a trimetallic unit

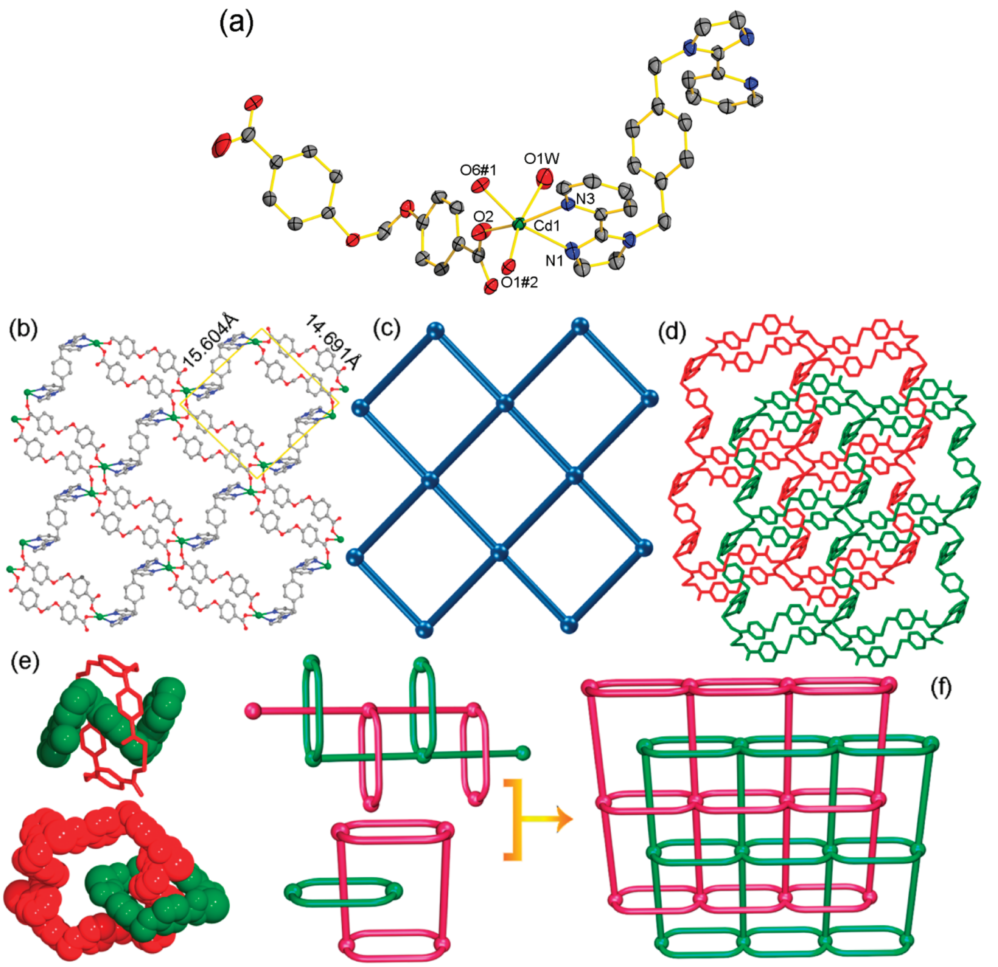

Figure 2. (a) Coordination environment of the Cd^{II} atom in **2** with the ellipsoids drawn at the 30% probability level; hydrogen atoms were omitted for clarity; (b) ball-and-stick representation of the sheet-like structure of compound **2**; (c) schematic view of the (4,4) topology of **2**; (d) ball-and-stick representation of interlocked nets; (e) the polyrotaxane and polycatenane motifs in **2**; (f) schematic description of the interlocked nets of **2**.

$[Zn_3(CO_2)_4(OH)_2]$. In addition, four $(L^3)^{2-}$ anions and four Zn^{II} ions (two Zn2 and two Zn3) assemble a large 56-membered ring $[Zn_4(L^3)_4]$ (Figure S3a, Supporting Information) with the Zn2$\cdots$Zn2 distance of 5.628 Å and Zn3$\cdots$Zn3 distance of 26.234 Å, respectively. The adjacent chains are pillared by bpib ligands with the bis-bidentate coordination mode in TTT conformation to generate a sheet (Figure 3b), showing a window with dimensions 13.117 Å by 17.358 Å. There is a parallelogrammic 50-membered ring $[Zn_4(L^3)_2(bpib)_2]$ (Figure S3b, Supporting Information) formed by two $(L^3)^{2-}$ anions, two bpib ligands, and four Zn^{II} ions with the distances for each edge and diagonal of 12.782, 12.839, 17.545, and 18.795 Å.

From the topological view, if each $[Zn_3(CO_2)_4(OH)_2]$ unit is considered as a 6-connected node, the Zn2 atom is considered as a 3-connected node, and the $(L^3)^{2-}$ anion and bpib ligand are considered as connectors, the structure of **3** is a (3,6)-connected net with $(4^3)(4^6\cdot6^6\cdot8^3)$ topology (Figure 3c). The potential windows formed by a single 2D network show incorporation of another identical network, thus giving a 2-fold parallel interpenetrating network (Figure 3d and Figure S3c, Supporting Information). Although the structure of **3** also shows both polyrotaxane and polycatenane character, it is different from those of compounds **1** and **2**; in **3**, each $[Zn_4(L^3)_4]$ loop is threaded by two bpib ligands as rods from the adjacent layers and the $[Zn_4(L^3)_4]$ ring and $[Zn_4(L^3)_2(bpib)_2]$ ring from adjacent layers interlock each other (Figure 3e,f). To the best of our knowledge, this is the first example of a 2-fold parallel interpenetrating network with a (3,6)-connected net showing both polyrotaxane and polycatenane character.

In addition, the coordination water molecule donates two hydrogen bonds to two adjacent carboxylate oxygen atoms (Table S2 and Figure S3d, Supporting Information), which forms a $[Zn_2(CO_2)_4(H_2O)_2]$ unit. If each $[Zn_2(CO_2)_4(H_2O)_2]$ unit is considered as a 4-connected node and the $[Zn_3(CO_2)_4(OH)_2]$ unit is also a 4-connected node, the structure of **3** is a 2-fold parallel interpenetrating network with (4,4) topology, which is similar to the structure of **2**.

---

(16) (a) Majumder, A.; Shit, S.; Choudhury, C. R.; Batten, S. R.; Pilet, G.; Luneau, D.; Daro, N.; Sutter, J.-P.; Chattopadhyay, N.; Mitra, S. *Inorg. Chim. Acta* **2005**, *358*, 3855. (b) Chen, W.; Yuan, H.-M.; Wang, J.-Y.; Liu, Z.-Y.; Xu, J.-J.; Yang, M.; Chen, J.-S. *J. Am. Chem. Soc.* **2003**, *125*, 9266. (c) Ganesan, S. V.; Natarajan, S. *Inorg. Chem.* **2004**, *43*, 198. (d) Zhang, J.-P.; Lin, Y.-Y.; Huang, X.-C.; Chen, X.-M. *Eur. J. Inorg. Chem.* **2006**, 3407. (e) Bourne, S. A.; Lu, J.; Moulton, B.; Zaworotko, M. J. *Chem. Commun.* **2001**, 861. (f) Sun, D.; Cao, R.; Liang, Y.; Shi, Q.; Su, W.; Hong, M. *J. Chem. Soc., Dalton Trans.* **2001**, 2335.

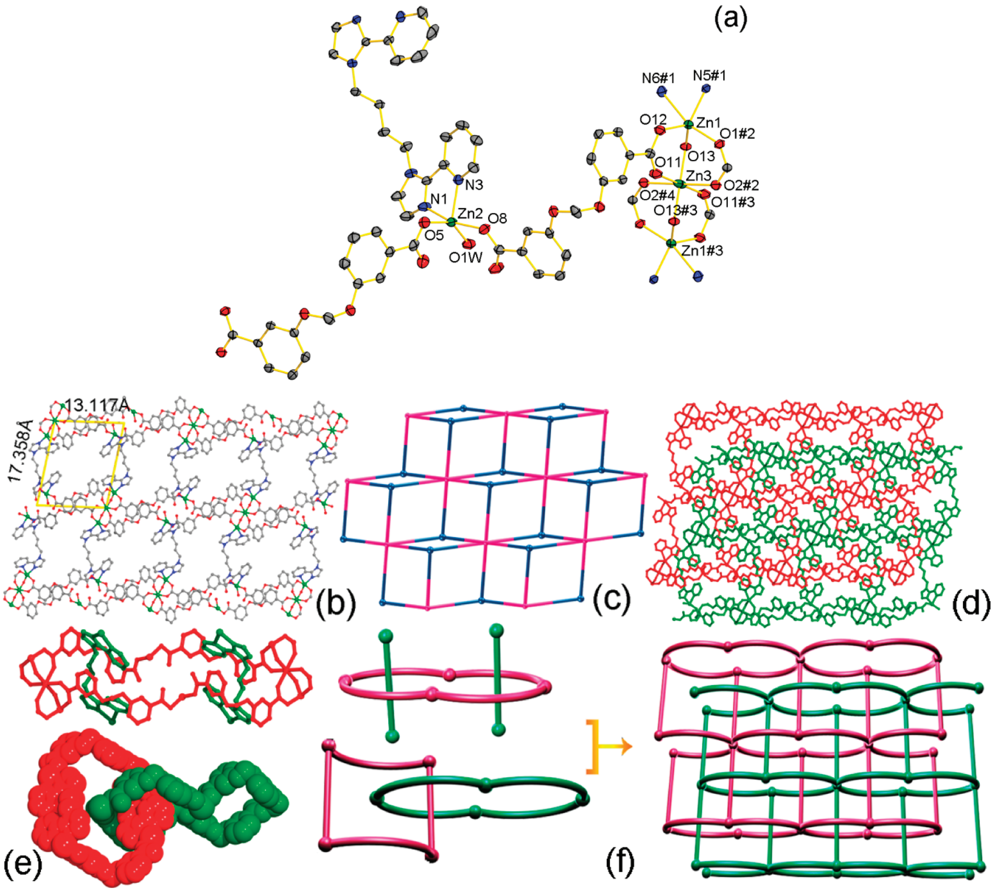

Figure 3. (a) Coordination environment of Zn^{II} atoms in **3** with the ellipsoids drawn at the 30% probability level; hydrogen atoms were omitted for clarity; (b) ball-and-stick representation of the sheet-like structure of compound **3**; (c) schematic view of the topology of **3**; (d) ball-and-stick representation of interlocked nets; (e) the polyrotaxane and polycatenane motifs in **3**; (f) schematic description of the interlocked nets of **3**.

Structural Description of 4. In order to investigate the influence of multicarboxylate ligands with different lengths on ultimate structures, the longer H_2L^4 is selected instead of H_2L^3, and compound **4** is obtained. The compound **4** shows a rare 2D→2D example with 3-fold parallel interpenetration of (4,4) layers. As shown in Figure 4a, the structure of **4** contains one kind of Zn^{II} atom and one kind of $(L^4)^{2-}$ and bpib ligands (Figure 4a). The Zn^{II} center is coordinated by three carboxylate oxygen atoms from different $(L^4)^{2-}$ ions and one nitrogen atom from the bpib ligand to give the ZnO_3N tetrahedral geometry. The $(L^4)^{2-}$ anions with the mono-and-bis(mono)-dentate coordination mode in the TGT-TGT conformation link Zn^{II} atoms to give a hinged chain containing the $[Zn_2(CO_2)_4]$ unit and a 40-membered ring, $[Zn_2(L^4)_2]$ (Figure S4a, Supporting Information) showing the corresponding edge and diagonal sizes of 10.455, 10.761, 13.956, and 15.982 Å. The bpib ligand with the bis-(mono)dentate coordination mode in the TTT conformation connects the adjacent chains to generate a 2D sheet (Figure 4b) with a window of dimensions 17.028 Å by 17.035 Å. There is a large 62-membered loop, $[Zn_4(bpib)_2(L^4)_2]$ (Figure S4b, Supporting Information), formed by four Zn^{II} ions, two bpib, and two $(L^4)^{2-}$ anions with the corresponding distances of 14.540, 17.035, 20.592, and 24.065 Å.

If each $[Zn_2(CO_2)_4]$ unit is considered as a 4-connected node and bpib and $(L^4)^{2-}$ anion are considered as linkages, the structure of **4** is a (4,4) topology (Figure 4c). Based on the large window in the sheet, the other two identical layers penetrate it in the parallel mode to form a 2D→2D 3-fold interpenetrating network (Figure 4d and Figure S4c, Supporting Information). It is interesting that this network also shows both polyrotaxane and polycatenane characters. The loop of $[Zn_2(L^4)_2]$ in one sheet is threaded by two bpib ligands as rods from two adjacent layers. A large ring of $[Zn_4(bpib)_2(L^4)_2]$ from one layer is interlocked by two $[Zn_2(L^4)_2]$ loops from the other two identical layers (Figure 4e,f).

When the Zn^{II} ion and bpib ligand are selected to react with H_2L^3 and H_2L^4, respectively, compounds **3** and **4** with different structural types have been obtained. Based on the different lengths for H_2L^3 and H_2L^4, they link Zn^{II} ions to form two kinds of hinged chains with different sized metal−multicarboxylate loops, which are connected by bpib ligands to form distinct structures of **3** and **4**. So they exhibit (3,6)-connected and 4-connected topological structures. H_2L^4 is longer than H_2L^3, so the structure of **4** shows a larger window than that in **3**, which can benefit formation of the higher degrees of interpenetrating network.

Structural Description of 5. X-ray crystallography has indicated that complex **5** is made up of one kind of Cd^{II} ion, one kind of bib ligand, and the $(L^4)^{2-}$ anion (Figure 5a). Cd^{II} exhibits a distorted octahedral coordination geometry surrounded by four carboxylate oxygen atoms from two $(L^4)^{2-}$ anions and two nitrogen atoms of different bib

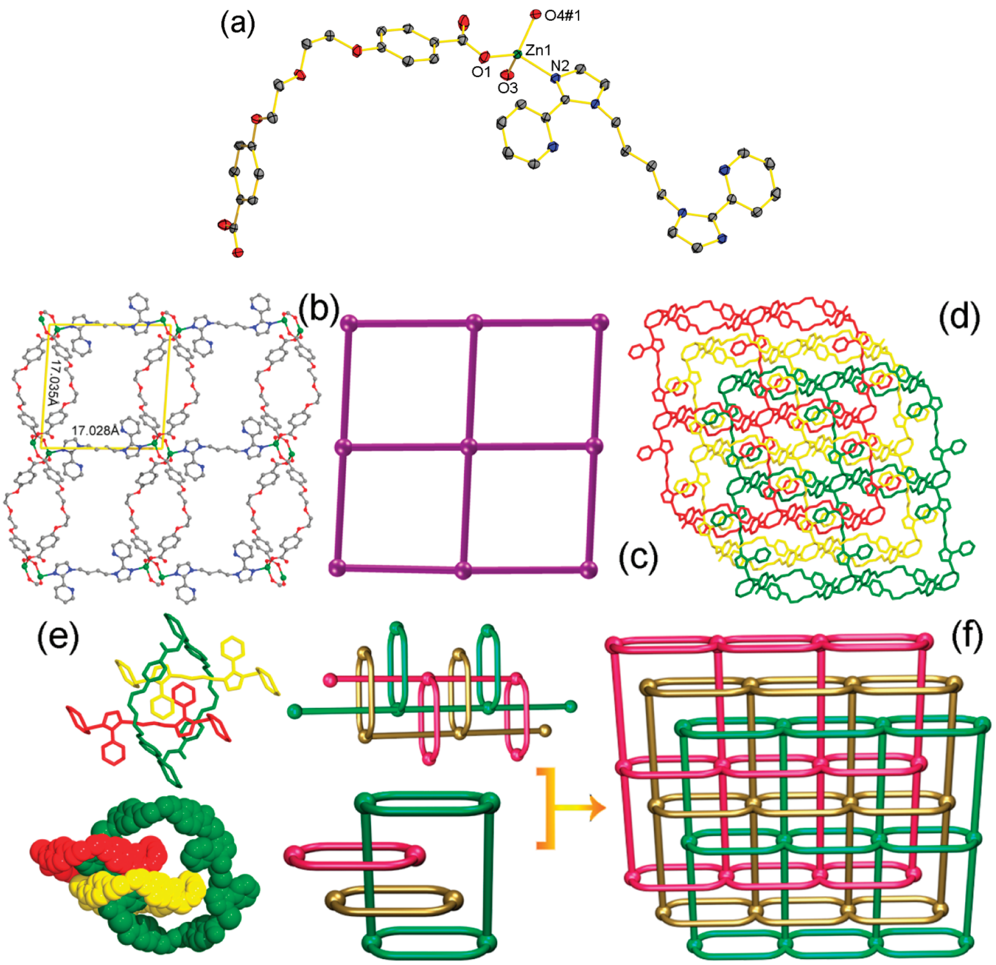

Figure 4. (a) Coordination environment of Zn^{II} atom in **4** with the ellipsoids drawn at the 30% probability level; hydrogen atoms were omitted for clarity; (b) ball-and-stick representation of the sheet-like structure of compound **4**; (c) schematic view of the (4,4) topology of **4**; (d) ball-and-stick representation of interlocked nets; (e) the polyrotaxane and polycatenane motifs in **4**; (f) schematic description of the interlocked nets of **4**.

molecules. The $(L^4)^{2-}$ anions coordinate Cd^{II} atoms with the bis-bidentate coordination mode in the TGTTTT (G = gauche) conformation to give a chain-like structure, which is pillared by the bib ligands with the TTT conformation to generate a 2D (4,4) sheet (Figure 5b) with a large grid, showing the dimensions 13.685 Å × 20.882 Å. The large grid allows each net to be penetrated by four other independent nets in parallel mode to form the interesting 2D 5-fold interpenetrating networks (Figure 5c and Figure S5, Supporting Information). It is interesting that the 2D 5-fold parallel interpenetrating networks show polycatenane character, in which there is a subunit formed by five rings from adjacent layers interlocking each other. This kind of connection mode is similar to the Olympic Rings (Figure 5d,e).

Due to different coordination modes of $(L^4)^{2-}$ anions, they link Cd^{II} to generate a single chain in **5** and a double chain in **4**, which are pillared by neutral ligands to form 5-fold and 3-fold interpenetrating networks, respectively. Comparison of the structures of **4** and **5** with those of **1**−**3** reveals more degrees of interpenetrating structures owing to the longer carboxylic acids in **4** and **5**.

Interpenetration phenomena are found to frequently occur during the self-assembly process.[17] But the 2D 5-fold parallel interpenetrating net is scarce. To the best of our knowledge, there are only two examples for 5-fold parallel interpenetrated (4,4) 2D layer frameworks. One of them is a covalently connected net within the structure of the coordination polymer $[Co(NCS)_2$(2,5-bis(4-pyridylethynyl) thiophene)].[18] The other is the 5-fold interpenetrated 2D hydrogen-bonded rhomboid grid supramolecular architectures with the compositions of $\{[Co(Hdpa)_2(BPDC)_2]\cdot 2H_2O\}$ or $[Zn(dpa)_2(HBPDC)_2]$.[19] So the structure of **5** is another example of 5-fold (4,4) 2D wavy layers formed by parallel interpenetration, which could help us deeply understand the nature of coordination polymer frameworks and better design functional materials.

As mentioned above, compounds **1**−**4** show both polyrotaxane and polycatenane character and various topological structures by changing carboxylic acids with different lengths, which mean that there are two kinds of motifs in compounds **1**−**4**, rotaxane-like species and catenated arrays. Notably, the rotaxane-like motif in compound **1** is formed by the metal−neutral ligand subunit as the loop and the carboxylate ligand as a rod threading the above loop. In **2**−**4**, the ring composition is the metal−carboxylate ligand, and

---

(17) Carlucci, L.; Ciani, G.; Macchi, P.; Proserpio, D. M.; Rizzato, S. *Chem.—Eur. J.* **1999**, *5*, 237.

(18) Son, S. U.; Kim, B. Y.; Choi, C. H.; Lee, S. W.; Kim, Y. S.; Chung, Y. K. *Chem. Commun.* **2003**, 2528.

(19) Montney, M. R.; Supkowskib, R. M.; LaDuca, R. L. *CrystEngComm* **2008**, *10*, 111.

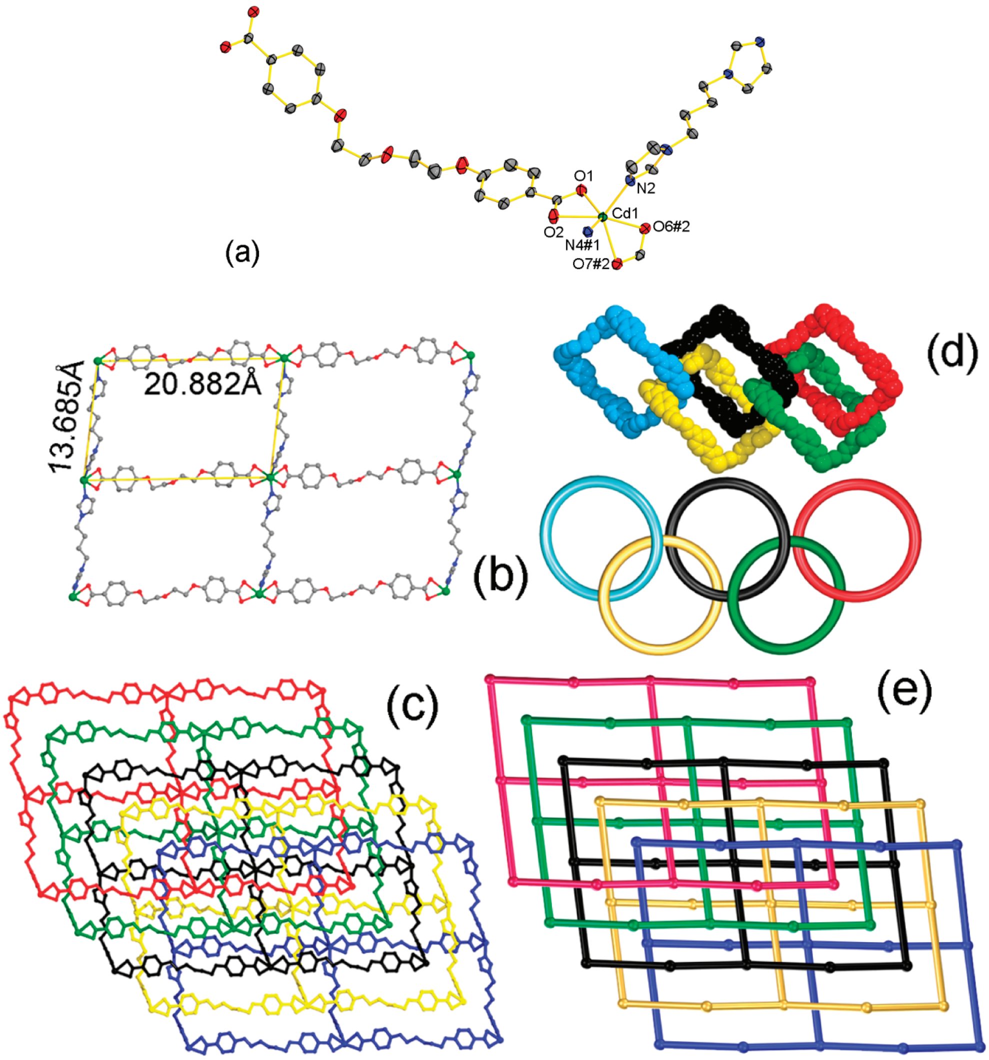

Figure 5. (a) Coordination environment of Cd^{II} atom in **5** with the ellipsoids drawn at the 30% probability level; hydrogen atoms were omitted for clarity; (b) ball-and-stick representation of the sheet-like structure of compound **5**; (c) ball-and-stick representation of 5-fold penetrating nets; (d) the polycatenane motifs in **5**; (e) schematic description of the 5-fold penetrating nets of **5**.

the corresponding rod is the neutral ligand. The carboxylate anions show the mono-and-bis(mono)-dentate coordination modes and coordinate to three metal centers in **2**−**4**, which benefit the formation of various metal−carboxylate chains with two or three metal−oxygen clusters. These chains are pillared by neutral ligands to generate the final different topological structures. Compound **2** shows a 2-fold parallel interpenetrating network with the (4,4) topology. When different angular H_2L^3 is selected to replace H_2L^2, compound **3** exhibits a 2-fold parallel interpenetrating network with the (3,6)-connected topology. Compared with the structure of **3**, **4** displays a 3-fold parallel interpenetrating network with the (4,4) topology by using the longer H_2L^4. The coordination modes of carboxylic anions in **2**−**4** play important roles in forming the special structures with both polyrotaxane and polycatenane characters.

In **4**, the $(L^4)^{2-}$ anion with the mono-and-bis(mono)-dentate coordination mode coordinates to metal centers in the TGTTGT conformation with the M···M (metal center) distance of 15.982 Å. Different from **4**, in **5**, the $(L^4)^{2-}$ anion with the bis-bidentate coordination mode coordinates to metal centers in the TGTTTT conformation with the M···M distance of 20.882 Å, which is longer than that of **4**. From a theoretical view, the longer the distance between two metal centers coordinated by one carboxylic anion is, the more the number of identical interpenetrating nets may be. The 3-fold parallel interpenetrating net of compound **4** and the 5-fold one of compound **5** support this view well.

Four kinds of carboxylic ligands with different lengths and angles adopt various coordination modes and conformations in **1**−**5** (Scheme 1). In addition, many factors, such as the radii of metal cations, the versatilities of the metal coordination geometries, and the donor characters of nitrogen atoms to the metals, play fundamental roles in the formation of the final products. These factors work together and have a significant effect on the structures of the coordination polymers. It is a feasible method to introduce ligands to construct coordination polymers with different structural types.

Luminescent Properties. Luminescent compounds are of great current interest because of their various applications in chemical sensors, photochemistry, and electroluminescent display.[20] The luminescent properties of zinc and cadmium carboxylate compounds have been investi-

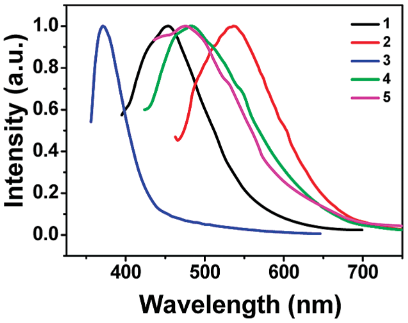

Figure 6. Solid-state photoluminescent spectra of **1**−**5** at room temperature.

Scheme 1. Schematic View of Five Compounds in This Work

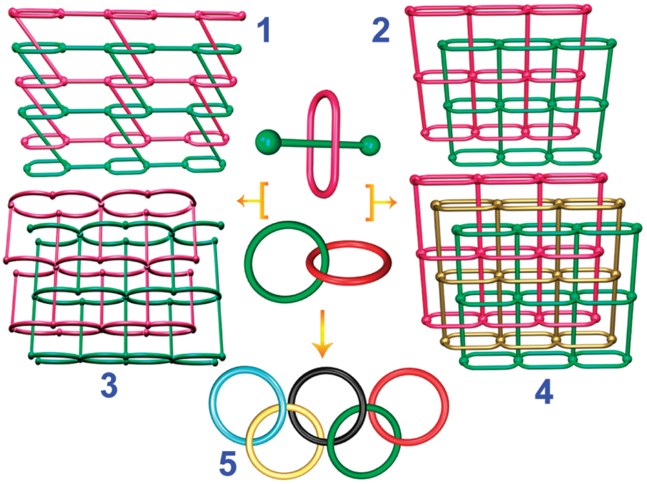

Table 2. The Wavelengths of the Emission Maximums and Excitation (nm)

	ligand			
	bimb	bpimb	bpib	bib
λ_{em}	432	360, 506	532	436
λ_{ex}	255	320	370	380

	compound				
	1	**2**	**3**	**4**	**5**
λ_{em}	451	537	369	481	475
λ_{ex}	375	440	335	400	400

gated.[21] The photoluminescent spectra of compounds **1**−**5** and N-donor ligands have been measured at room temperature (Figure 6),and the wavelengths of the emission maximums and excitation are listed in Table 2 for compounds **1**−**5** and N-donor ligands. And solid H_2L^1−H_2L^4 ligands are nearly nonfluorescent in the range 400−800 nm at ambient temperature. In comparison with the N-donor ligands, the emission maximums of compounds **1**−**5** have changed. This may be caused by the following reasons: The emission peaks for **1** may arise from $\pi^* \rightarrow \pi$ transitions of the bimb ligands because a similar peak also appears for the free bimb ligand, which is similar to the previous literature.[22] The emissions of compounds **2**−**4** may be attributed to a joint contribution of the intraligand $\pi^* \rightarrow \pi$ transitions, which effectively increase the rigidity of the ligand and reduce the loss of energy by nonradiative decay, and charge transfer transitions between the coordinated ligands and the metal center.[11a,e]

Thermal Analyses. In order to characterize the compounds more fully in terms of thermal stability, their thermal behaviors were studied by TGA. The experiments were performed on samples consisting of numerous single crystals of **1**−**5** under N_2 atmosphere with a heating rate of 10 °C/min. The results of the TGA for compounds **1**−**5** are shown in Figure S6 in the Supporting Information.

For **1**, the weight loss begins with decomposition starting at 273 °C and ending above 489 °C. The remaining weight of 21.1% corresponds to the percentage (20.7%) of CdO. For compounds **2** and **3**, the weight losses in the range of 20−151 °C for **2** and 15−98 °C for **3** correspond to the removal of the corresponding coordination water molecules. The anhydrous compositions begin to decompose at 203 °C ending above 487 °C for **2** and at 182 °C ending above 479 °C for **3**. The remaining weight corresponds to the formation of CdO in **2** (obsd 21.2%, calcd 21.0%) and ZnO in **3** (obsd 18.5%, calcd 18.3%). The anhydrous compounds **4** and **5** begin to decompose at 216 °C for **4** and 187 °C for **5** and end above 537 °C for **4** and 527 °C for **5**. The remaining weight of 14.5% for **4** and 18.6% for **5** correspond to the percentage (14.0%) of ZnO in **4** and (19.9%) of CdO in **5**.

Conclusion

In summary, we have synthesized five mixed-ligand coordination complexes under hydrothermal conditions. Compounds **1**−**4** display 2D→2D parallel interpenetrating structures with various topological types and show both polyrotaxane and polycatenane character. Compound **5** is a 5-fold parallel interpenetrating net with (4,4) topology. By careful inspection of these structures, we find that different topological structures have been achieved with the increase of carboxylic ligand length. It is believed that various carboxylic ligands and N-donor ligands with different coordination modes and conformations are important for the formation of the different structures. These results suggest that novel extended entanglements containing both polyrotaxane and polycatenane character can be realized by combining metal nodes with flexible N-donor ligands and various carboxylic ligands. Investigations in this direction are currently under way.

Acknowledgment. The authors gratefully acknowledge the financial support from the National Natural Science Founda-

---

(20) (a) Wu, Q.; Esteghamatian, M.; Hu, N.-X.; Popovic, Z.; Enright, G.; Tao, Y.; D'Iorio, M.; Wang, S. *Chem. Mater.* **2000**, *12*, 79. (b) McGarrah, J. E.; Kim, Y.-J.; Hissler, M.; Eisenberg, R. *Inorg. Chem.* **2001**, *40*, 4510. (c) Santis, G. D.; Fabbrizzi, L.; Licchelli, M.; Poggi, A.; Taglietti, A. *Angew. Chem., Int. Ed. Engl.* **1996**, *35*, 202.

(21) Zheng, S.-L.; Yang, J.-H.; Yu, X.-L.; Chen, X.-M.; Wong, W.-T. *Inorg. Chem.* **2004**, *43*, 830.

(22) (a) Zheng, S.-L.; Zhang, J.-P.; Chen, X.-M.; Huang, Z.-L.; Lin, Z.-Y.; Wong, W.-T. *Chem.—Eur. J.* **2003**, *9*, 3888. (b) Kang, Y.; Zhang, J.; Li, Z.-J.; Cheng, J.-K.; Yao, Y.-G. *Inorg. Chim. Acta* **2006**, *359*, 2201. (c) Guo, Z.; Cao, R.; Li, X.; Yuan, D.; Bi, W.; Zhu, X.; Li, Y. *Eur. J. Inorg. Chem.* **2007**, 742.

tion of China (Project Nos. 20573016 and 20703008), the National High-tech Research and Development Program (863 Program 2007AA03Z354), Program for Changjiang Scholars and Innovative Research Team in University (Grant IRT0714), and the Science Foundation for Young Teachers of Northeast Normal University (No. 20070309).

Supporting Information Available: X-ray crystallographic files (CIF), additional figures, selected bond distances and angles, and TGA curves of compounds **1**−**5**. This material is available free of charge via the Internet at http://pubs.acs.org.

IC801275W